ID: 137

MODELING AND ANALYSIS OF A TRANSCRITICAL RANKINE POWER CYCLE WITH A LOW GRADE HEAT SOURCE

NGUYEN C., VEJE C.
Mads Clausen Institute, University of Southern Denmark, Alsion 2, DK-6400, Denmark
chngu@mci.sdu.dk, veje@mci.sdu.dk

ABSTRACT

A transcritical carbon dioxide (CO_2) Rankine power cycle has been analyzed based on first and second law of thermodynamics. Detailed simulations using distributed models for the heat exchangers have been performed in order to develop the performance characteristics in terms of e.g., thermal efficiency, exergetic efficiency and specific net power output. A generic cycle configuration has been used for analysis of a geothermal energy heat source. This model has been validated against similar calculations using industrial waste heat as the energy source. Calculations are done with fixed temperature and mass flow of the heat source.
The results show the existence of an optimum high pressure for maximizing performance and for minimizing the heat transfer area. The exergy analysis specifies points of potential improvement in the heat exchanger temperature match and points to optimal operating conditions for the high side pressure. In addition the results underline that the investment cost for additional heat exchange components such as an internal heat exchanger may be unprofitable in the case where the heat source is free.

1. INTRODUCTION

According to the report *International Energy Outlook 2009* published by The Energy Information Administration (EIA, 2009) the global demand for electricity will continue to increase in the coming years. The world electricity generation in 2006 was 18 trillion kilowatt-hours, with 19% being from renewable energy, 15% from nuclear and 66% from fossil fuels (natural gas, coal and oil). In 2030 the total electricity generation is predicted to increase by 77%. In the same period the electricity generation from renewable energy, nuclear energy and fossil fuels is predicted to increase by 97%, 41% and 85% respectively.

These figures indicate that it could be appropriate, not only to adopt more renewable and alternative energy sources, but also to optimize the conversion efficiency. Here we focus on a geothermal energy source validated against an alternative energy source of waste heat from industry.

Geothermal energy is widely available in some parts of the world, but the low conversion efficiency makes it uneconomic compared to other fuels (DiPippo R, 2008), (Lee K.C, 2001) and (Yari 2010). For industrial waste heat, EIA (2009) reports that 18% of the total energy consumption is due to the chemicals and iron-steel industries. For example eight of the largest Canadian manufacturing sectors release approximately 70% of their energy input to the environment as heat (Galanis et al., 2009).

The common issue for these energy sources is the high quantity but low quality due to the low temperature relative to conventional furnace temperatures. For conversion to electricity a power cycle that is appropriate for low temperature heat sources has to be adopted. One of these is the CO_2 transcritical Rankine power cycle (CTRPC) see e.g. (Cayer et al., 2009), (Chen et al., 2006), (Galanis et al., 2009) and (Zhang et al., 2007), which is the cycle to be analyzed in this paper. We will be using an energy and exergy analysis on the components in conjunction with a distributed model for the heat exchangers.

2. SYSTEM AND CYCLE MODEL

The system to be considered is of a generic configuration as illustrated in Figure 1 (left). The configuration consists of five components: evaporator, turbine, internal heat exchanger (IHX), condenser and pump. If the effectiveness of the IHX is set to zero, the configuration will be like the basic Rankine power cycle without

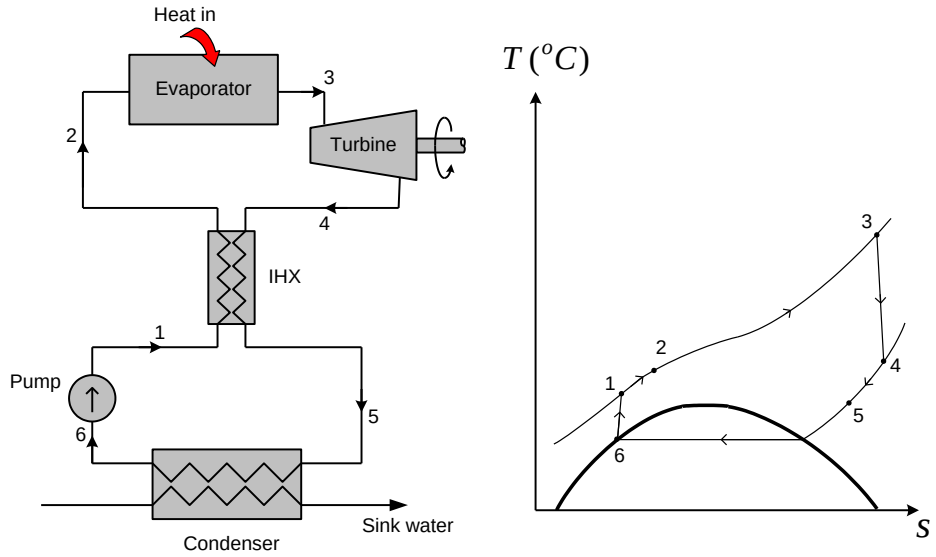

Figure 1. Left: The generic configuration for the Transcritical Rankine Power Cycle (TRPC). Right: Cycle in T-s diagram with corresponding state points.

internal heat exchange such that a comparison between two different system configurations can be made by simply changing one parameter. The corresponding thermodynamic cycle is shown in a temperature – entropy diagram in Figure 1 (right). The state points from the component diagram are also indicated. These will be used in the model equations outlined below.

The main assumptions of the model are:

- The cycle is always transcritical.
- Steady state flow in the whole cycle.
- The kinetic and potential energy change as well as the heat and friction losses are neglected.
- The isentropic efficiencies of the turbine and the pump are set to 0.8
- The effectiveness of the IHX is set to 0.9.
- The inlet temperature of the cooling water is 10°Celsius.
- At the exit of the condenser saturated liquid is supposed and temperature is 15°Celsius.

2.1. Energy Analysis

In order to determine the 1.law thermal efficiency η_{th} and the specific net output w we apply a conventional energy analysis of the cycle. It is based on the first law of thermodynamics and on the assumptions listed above. The equations governing for the different components are listed below (Cengel and Boles, 1998). h refers to the state point enthalpies, $\dot{m}$ to mass flows, η to efficiencies, $\dot{W}$ to power and $\dot{Q}$ to heat flows. Subscripts should be self-explanatory. For the pump and turbine efficiency and power we have:

$$\eta_{pum} = \frac{h_{1,is} - h_6}{h_1 - h_6}, \tag{1}$$

$$\dot{W}_{pum} = \dot{m}_{CO2}\left(h_1 - h_6\right), \tag{2}$$

$$\eta_{tur} = \frac{h_3 - h_4}{h_3 - h_{4,is}}, \tag{3}$$

$$\dot{W}_{tur} = \dot{m}_{CO2}\left(h_3 - h_4\right). \tag{4}$$

For the evaporator, condenser and IHX:

$$\dot{Q}_{in} = \dot{m}_{CO2}\left(h_3 - h_2\right), \tag{5}$$

$$\dot{Q}_{out} = \dot{m}_{CO2}\left(h_5 - h_6\right), \tag{6}$$

$$\eta_{pum} = \frac{h_{1,is} - h_6}{h_1 - h_6}, \tag{7}$$

$$\dot{Q}_{\max} = \dot{m}_{CO2}\left(h_4 - h_{5(T_5=T_1)}\right), \tag{8}$$

$$\eta_{IHX} = \frac{\dot{m}_{CO2}\left(h_4 - h_5\right)}{\dot{Q}_{\max}}. \tag{9}$$

And finally we determine the first law thermal efficiency,

$$\eta_{th} = \frac{\dot{W}_{tur} - \dot{W}_{pum}}{\dot{Q}_{in}}, \tag{10}$$

and the specific power output *w*

$$w = \frac{\dot{W}_{out}}{\dot{m}_{CO2}}, \tag{11}$$

which completes the system of equations for the energy analysis.

2.2. Exergy Analysis

In order to consider the quality of the heat exchange in the evaporator, the IHX and the condenser an exergy analysis is performed. This analysis is based on the second law of thermodynamics, with the objectives to determine the exergetic efficiency of the cycle and the fractional exergy destruction in each component of the configuration.

In contrast to the thermal efficiency, the exergetic efficiency depend on the mass flow rates of the working fluid, the cooling water and the heat source fluid. Defining $F = (\dot{W}_{tur} - \dot{W}_{pum})/\dot{W}_{\max}$ and combining with eq. (11) the mass flow rate of the working fluid can be found by

$$\dot{m}_{CO2} = \frac{F \cdot \dot{W}_{\max}}{w} \tag{12}$$

where $\dot{W}_{\max}$ is the maximum theoretical power produced by a Carnot engine operating at the temperature of the inlet of the heat source $T_{hs,in}$ and the inlet of the sink $T_{\text{sink},in}$. From the Carnot efficiency, $\eta_{carnot} = 1 - \left(T_{\text{sink},in}/T_{hs,in}\right) = \dot{W}_{\max}/\dot{Q}_{in,\max}$, and since $\dot{Q}_{in,\max} = \dot{m}_{hs} C_{P,hs}\left(T_{hs,in} - T_{\text{sink},in}\right)$, we find

$$\dot{W}_{\max} = \dot{m}_{hs} C_{P,hs}\left(T_{hs,in} - T_{\text{sink},in}\right)\left(1 - \left(T_{\text{sink},in}/T_{hs,in}\right)\right). \tag{13}$$

$\dot{m}_{CO2}$ and $\dot{m}_{hs}$ can then be found by solving equation (12) and (13) simultaneously.

In the condenser two situations can occur depending on the state of the CO_2 at the outlet of the IHX (state point 5). First the CO_2 can be superheated, which divide the condenser into a single-phase region and a two-phase region as shown in Figure 2. In this situation, a pinch of 3℃ at the saturated vapour point ($T_{5'}$) of the CO_2 is assumed to prevent the temperature profiles (CO_2 and water) to intersect, i.e.

$$T_{5'} = T_{\text{sink},as} + 3 \tag{14}$$

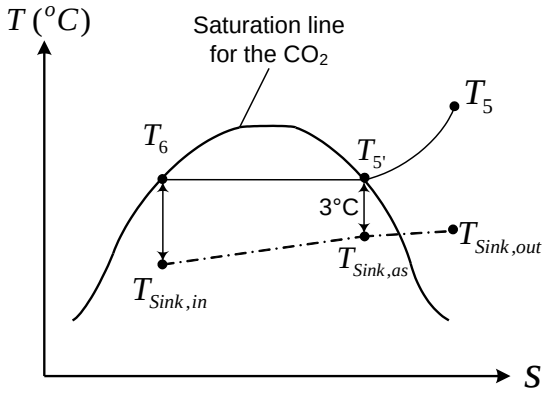

Figure 2. Temperatures at the condenser.

In the two-phase region the energy balance equation become

$$\dot{m}_{CO2}\left(h_{5'}-h_6\right)=\dot{m}_{\text{sink}}C_{P,\text{sink}}\left(T_{\text{sink,as}}-T_{\text{sink,in}}\right), \tag{15}$$

and the global energy balance become

$$\dot{m}_{CO2}\left(h_5-h_6\right)=\dot{m}_{\text{sink}}C_{P,\text{sink}}\left(T_{\text{sink,out}}-T_{\text{sink,in}}\right). \tag{16}$$

In the second situation state point 5 falls in the two-phase region. Eq. (15) can then be ignored and the water mass flow rate can be calculated by eq. (16). In this situation $T_{sink,out}$ will be equal to $T_{sink,as}$, since $h_{5'}$ is equal to h_5.

With the preceding assumptions the specific flow exergy is given by

$$e=h-h_0-T_0(s-s_0), \tag{17}$$

where the subscript 0 refers to the *dead state* assumed to be at 10℃ and 0.1013MPa (atmospheric pressure). The exergy destruction rates for each component can then be calculated by

$$\dot{E}_d=\sum_i \dot{m}_{in}e_{in}-\sum_o \dot{m}_{out}e_{out}-\dot{W}, \tag{18}$$

and the total exergy destruction is the sum of the individual contributions

$$\dot{E}_{d,tot}=\dot{E}_{d,pum}+\dot{E}_{d,tur}+\dot{E}_{d,eva}+\dot{E}_{d,con}+\dot{E}_{d,IHX}, \tag{19}$$

where the subscripts refers to the pump, turbine, evaporator, condenser and the IHX respectively. The overall exergetic efficiency can then be found by:

$$\eta_{ex}=1-\frac{\dot{E}_{d,tot}}{\dot{m}_{hs}\cdot\dot{e}_{hs,in}}. \tag{20}$$

2.3. Heat exchanger model

The heat exchangers are all assumed to be of the *shell and tube counter-flow* type. For calculations on such heat exchangers the logarithmic mean temperature difference (LMTD) method is widely used to find UA values for the overall heat transfer. This method is however based on the assumption of constant thermodynamic properties over the whole heat exchanger. However, it is well known that the thermal properties for CO_2 changes dramatically during heat exchange near the critical point and that a distributed model is necessary (Cayer et al., 2009). Thus, the LMTD method is modified by discretising the heat exchangers in sufficiently small sections so that the assumption of constant properties can be valid as shown

in Figure 3. In each section an average value for the properties can then be used and a ΔUA-value is calculated. The total UA is the sum of the ΔUA's in each section.

Using the LMTD-method on a small section as illustrated in Figure 3 the energy balance equations become (Cengel, 2003):

$$\Delta\dot{Q} = \dot{m}_{f1}\left(h_{f1}^{in} - h_{f1}^{out}\right), \tag{21}$$

$$\Delta\dot{Q} = \dot{m}_{f2}\left(h_{f2}^{out} - h_{f2}^{in}\right), \tag{22}$$

and

$$\Delta\dot{Q} = \Delta UA\frac{\left(T_{f1}^{in} - T_{f2}^{out}\right) - \left(T_{f1}^{out} - T_{f2}^{in}\right)}{\ln\left[\left(T_{f1}^{in} - T_{f2}^{out}\right)/\left(T_{f1}^{out} - T_{f2}^{in}\right)\right]}. \tag{23}$$

These equations are generic for the IHX, evaporator, and condenser.

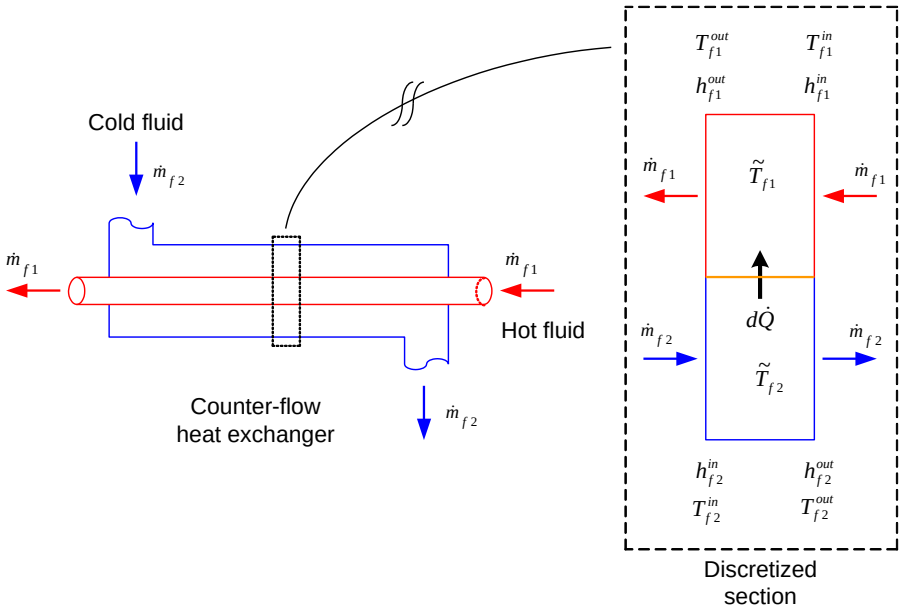

Figure 3. Discretising the counter-flow heat exchanger.

3. RESULTS AND DISCUSSION

The equations specified in section 2 are implemented in EES V.8.629 (Klein 2009). It is an equation solver with built in fluid properties, where the fluids: real air, *Air_ha* is used for the industrial waste heat, *water* is used for geothermal heat and condenser secondary side and *R744* is used for CO_2. The model has been verified against published results for an analysis of a transcritical power cycle for use with industrial waste heat (Cayer et al., 2009). The fixed parameters for the verification are presented in Table 1 and are the same as in Cayer et al. (2009) for comparison. The variable parameters are the high pressure P_3(9-15MPa), the fractional maximum power output F (0.15 and 0.20) and the efficiency of the IHX η_{IHX} (0 and 0.9).

Table 1.Fixed parameters for model verification.

	$\dot{m}_{hs}$ [kg/s]	P_{hs} [MPa]	$T_{hs,in}$ [C]	T_3 [C]	$T_{\sin k,in}$ [C]
Verification	314.5	0.1013	100	$0.95\cdot T_{hs,in}$	10
This model	1	1.002	180	$0.95\cdot T_{hs,in}$	25

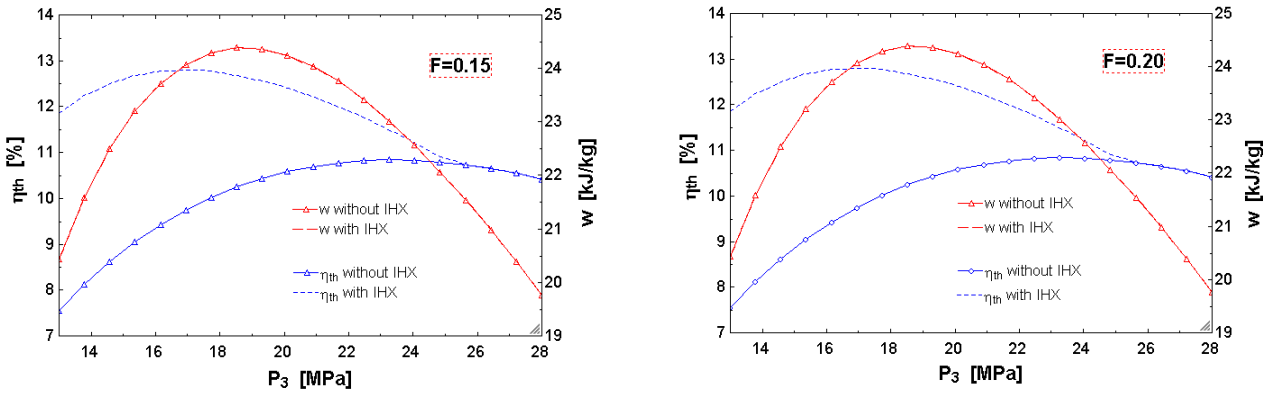

Figure 4. Left: Thermal efficiency η_{th}. Right: specific output w with and without IHX for F =0.15 and for F =0.20.

The parameters kept constant for this study are also presented in Table 1. The variable parameters are again the high pressure P_3 (15-27MPa), the fractional maximum power output, F (0.15 and 0.20) and the efficiency of the IHX, η_{IHX} (0 and 0.9).

Figure 4 shows the thermal efficiency η_{th} and the specific net output w versus the high pressure P_3 for F = 0.15 and F = 0.20 respectively. The two figures show that η_{th} and w do not depend on F. w has a maximum value of 24.4 kJ/kg at P_3 = 18.5 MPa and these values are the same with and without the IHX. With the IHX, η_{th} has a higher maximum value than without the IHX. Also the maximum thermal efficiency occurs at a lower pressure. This maximum without the IHX is 10.8% at a pressure of 23.3MPa whereas it is 12.8% at 16.9MPa with the IHX. The pressure which maximizes w is not the same that maximizes η_{th}. Note that from around P_3 = 25.0 MPa, the effect of the IHX vanishes since T_4 and T_1 becomes equal.

Increasing F will of course increase the net power output $\dot{W}_{out}$, but there is an upper limit. As F increase, the temperature of the outlet of the heat source T_{hs} decrease and approaches T_2. Since $T_{hs,out}$ cannot become lower than T_2 there is an upper limit for F. For the given conditions this limit is near 0.227, which correspond to a maximum power output of 53.0 kW.

Figure 5 shows in opposition to the results of the energy that the exergetic efficiency η_{ex} *does* depend on F. Increasing F will decrease η_{ex}. This mean that the more power extracted from the cycle will result in more total exergy destruction.

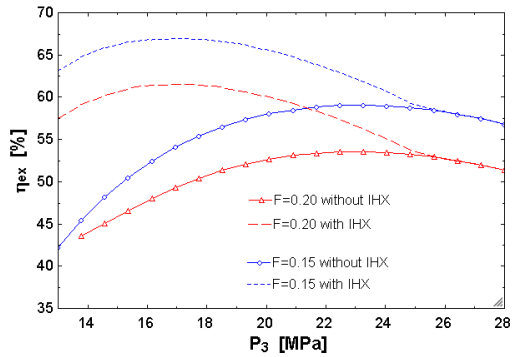

Figure 5. Exergetic efficiencies η_{ex} with and without IHX for $F = 0.15$ and $F = 0.20$.

The IHX has a similar effect on η_{ex} as on η_{th}, that is, using the IHX will decrease the optimal high side pressure and the efficiencies will increase. The pressures that maximize the exergetic efficiency η_{ex} for the two values of F are almost the same. Without the IHX, η_{ex} has a maximum of 59.1% for F =0.15 and 53.6% for F =0.20 at 23.3 MPa. Including the IHX, η_{ex} has a maximum of 67.0% for F =0.15 and 61.5% for F =0.20 at 16.9 MPa.

We can determine the fractional exergy destruction of each component through

$$\beta_{comp} = \frac{\dot{E}_{d,comp}}{\dot{E}_{d,tot}}, \tag{24}$$

where subscript *comp* refers to the individual components. Investigating the distribution of β at the optimal P_3 for maximum η_{ex} we find that most of the destructions occur at the turbine and the evaporator. The large exergy destruction at the evaporator indicates a poor temperature matching between the heat source and the working fluid. Efforts should be made to improve this match to increase the power output.

Figure 6 (left) shows P_3 versus the UA-values for each heat exchanger and P_3 versus the total UA-values (right). Each curve shows a minimum UA value. For $F = 0.15$ without IHX the minimum UA_{total} is 60.6 kW/K at P_3 =19.3 MPa. With the IHX the minimum UA_{total} values are approximately 6-8 kW/K higher at approximately 2 MPa lower pressures. Thus adding an IHX does not reduce UA_{Eva} sufficiently to reduce UA_{total}. Increasing F will also increase UA_{total}, but the pressure for the minimum are almost the same.

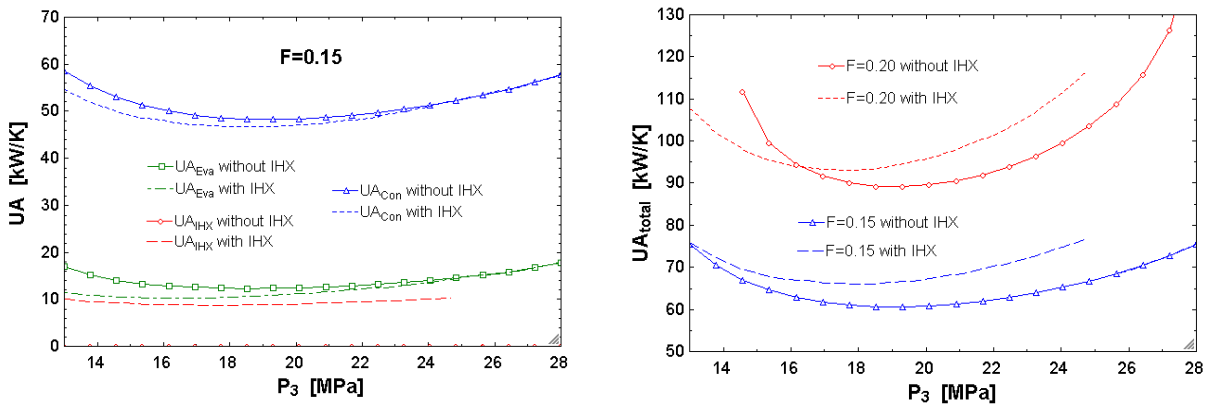

Figure 6. Left: UA-value for each of the three heat exchanger with and without IHX for $F = 0.15$. Right: Total UA-value for all heat exchangers with and without IHX for $F = 0.15$ and for $F = 0.20$.

From the calculation of the UA values the surface area A can be calculated using suitable correlations for the overall heat transfer coefficient. This is done in (Cayer et al., 2009), where it shows that the minimum surface areas also exist, and these are at almost same pressure for the minimum UA's. Since the surface area is a good indication of the cost of a heat exchanger, it is wise to dimension and operate at the pressure (optimal pressure) with minimum UA and A. The optimal pressure for minimum UA and A is close to the optimal pressure for getting the maximum power output.

4. CONCLUSIONS

In this paper the CO_2 transcritical Rankine power cycle (CTRPC) has been analyzed based on the first and second law of thermodynamic and based on a modified log mean temperature difference (LMTD) method to model the performance characteristics. A generic CTRC configuration has been modeled for two different

types of heat sources: Industrial waste heat and geothermal heat. The thermal efficiency η_{th}, the exergetic efficiency η_{ex}, the specific net output w, the total heat transfer product were the performance characteristics investigated.

Common performance characteristics of the heat sources are the following:

- There exists an optimum (design) pressure $P_{3,opt}$ for maximum η_{th}, η_{ex} and w, and for minimum UA_{total}. These values have not the same $P_{3,opt}$.
- The value of $\dot{W}_{out}$ does not affects η_{th} and w but affects η_{ex} and UA_{total}.
- The internal heat exchanger (IHX) has no effect on w but provides a lower $P_{3,opt}$ for maximum η_{th} and η_{ex}. The IHX increases the maximum η_{th} and η_{ex} only slightly.
- There is an upper limit for the power output $\dot{W}_{out}$.
- η_{ex} decreases with increase $\dot{W}_{out}$.
- Increasing the heat sources temperature will increase the maximum η_{th}, η_{ex} and UA_{total} and the corresponding $P_{3,opt}$ will also increase.

Since the IHX has no effect on either w or $\dot{W}_{out}$ but increases UA_{total} the use of it is not recommended. It does improve η_{th} and η_{ex}, but since the heat sources are a free, the focus should be on maximizing $\dot{W}_{out}$ and not η_{th} and η_{ex}.

5. REFERENCES

Cayer E, Galanis N, Désilets M, Nesreddine H, Roy P. 2009, Analysis of a carbon dioxide transcritical power cycle using a low temperature source, Applied Energy 86: 1055– 1063.

Cengel Y. A, Boles M. A. 1998, Thermodynamics 3.editio,. McGraw Hill.

Cengel Y. A. 2003, Heat transfer 2.edition, McGraw Hill.

Chen Y, Lundqvist P, Johansson A, Platell P. 2006, A comparative study of the carbon dioxide transcritical power cycle compared with an organic rankine cycle with R123 as working fluid
in waste heat recovery, Applied Thermal Engineering 26: 2142–2147.

DiPippo R. 2008, Geothermal Power Plants 2. Edition, Elsevier Ltd.

Energy Information Administration (EIA). 2009, International Energy Outlook 2009, www.eia.doe.gov.

Galanis N, Cayer E, Roy P, Denis E.S and Désilets M. 2009, Electricity generation from low temperature sources, Journal of Applied Fluid Mechanics 2: 55-67.

Klein S.A. 2009, Engineering equation solver (EES), Academic Commercial V8.4 McGraw Hill.

Lee K.C. 2001. Classification of geothermal resources by exergy, Geothermics 30:431-442.

Zhang X.R, Yamaguchi H, Fujima K, Enomoto M, Sawada N. 2007, Theoretical analysis of a thermodynamic cycle for power and heat production using supercritical carbon dioxide, Energy 32: 591–599.

Yari M, 2010, Exergetic analysis of various types of geothermal power plants. Renewable Energy 35: 112–121.